Self-forced stabilization of inter-modal oscillation in multi-section semiconductor lasers at X-band

Tianchi Sun,[1] Ⓘ **Ajay K. Poddar,**[2] **Ulrich L. Rohde,**[2] **and Afshin S. Daryoush**[1,*]

[1]*Department of ECE, Drexel University, 3141 Chestnut Street, Philadelphia, PA 19104, USA*
[2]*Synergy Microwave Corporation, 201 McLean Boulevard, Paterson, NJ 07504, USA*
[*]*daryousa@drexel.edu*

Abstract: Forced oscillation based on self-injection locked phase-locked (SILPLL) opto-electronic oscillator (OEO) technique is the basis of highly stable and low phase noise oscillators to be used as a key component in modern communication and sensing systems. To avoid large-size modular OEO, inter-modal oscillation at X-band frequencies is achieved in a compact multi-mode multi-section semiconductor laser using InP foundry service. Self-forced oscillation technique of SILPLL is demonstrated, where a phase noise performance of −98 dBc/Hz is measured at 10 kHz offset carrier of 11 GHz, which is an improvement of 68 dB compared with the free-running condition, which corresponds with 600 times reduction in calculated timing jitters from the free-running case to reach 0.45 ps for over 1 kHz to 1 MHz bandwidth.

1. Introduction

Low phase noise RF sources are important part of coherent detection techniques in many RF applications, such as terrestrial and space communications. Traditional method of generating stable RF signals using highly stable crystal oscillator multiplication process [1] suffers from a higher prime power consumption, a larger size, poor AM noise, and higher AM-PM noise conversion compared with forced oscillation designs of injection locked phase locked loop technique [2]. In order to expand generation of very stable oscillation frequency to microwave frequencies range of X-band and K-band, electronically tuned opto-electronic oscillator (OEO) solutions are reported using yttrium iron garnet (YIG) coarse tuning combined with optimized optical delay in optical transversal filter for fine tuning [3–6]. Further direction of developing a compact size OEO at RF oscillator relies on chip level integration of dual mode lasers [7–8], using lasers with external cavity [9–10], and Si-photonics based integrated semiconductor laser [11]. There are two major methods for semiconductor laser based structures of using beat-notes of two symmetric lasers output [12–13] while another utilize inter-modal operation of multi-mode lasers [14–17]. The former method usually targets at hundreds of GHz range benefiting from high optical frequency [12]. Meantime, its linewidth is very poor which is around tens of megahertz [12–13]. On the other hand, second method using inter-modal output of multi-mode semiconductor laser usually targets efficiently at tens of GHz frequency range. Its performance using different locking methods are reported in [14–22] with maximum output frequency less than 40 GHz. However, in these publications, the performance of semiconductor laser inter-modal RF oscillation all depends on the purity of the external RF reference, as the RF free-running inter-modal oscillation signal has poor frequency stability.

In this paper, a DBR based multi-mode multi-section semiconductor laser is reported for RF output generation without utilizing any external reference; its design diagram is shown in Fig. 1, using different optical components from shared InP wafer run of SmartPhotonics foundry service [23]. There are four major sections of gain medium (SOA), phase modulation (PM), filtering

distributed Bragg reflector (DBR), and amplitude modulator (EAM) sections [24]. The SOA is fabricated by multi quantum well InGaAs/InP structure for operation at 1550 nm. The front and back DBR is functioned as reflection mirror filter [25] to form laser cavity, which its bandwidth affects the effective number of output modes in the multi-mode laser. For frequency tuning of RF signal output, material index variation of PM section [26] is employed using electro-optic property of InP by static bias condition variations. Meantime, its dynamic modulation plays an important role in phase locking process of RF signal over 50 MHz of bandwidth. Last, the EAM section outside the laser cavity controls laser modes by shifting edge of wavelength dependent absorption rate. The output of the laser is monitored in an optical spectrum analyzer and its intermodal oscillations are detected using an external high-speed photodetector (Discovery Semiconductor DSC50S) and displayed on RF phase noise analyzer. Besides the compact multi-mode laser chip design, novel forced technique of self-injection locking [27] and self-phase locking [28] are also employed in this paper for further reduction of the output phase noise and improving inter-modal oscillation frequency stability. Moreover, optimized delay line using self-injection locked triple phase-lock loop (SILTPLL) [29] is achieved with reported best phase noise performance without any external reference.
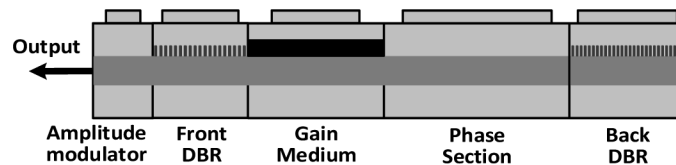
Fig. 1. Block diagram of inter-modal laser based RF synthesizer on a microchip structure.

2. Multi-mode laser and inter-modal RF oscillation

The design detail of multi-mode semiconductor DBR laser is shown in Fig. 2. The length of DBR back mirror and DBR front mirror is 600 μm and 200 μm separately. Phase section length is designed with 1250 μm while SOA is 800 μm. Different section is connected by shallow etched waveguide to form the complete laser cavity. The total cavity length (including connecting waveguide) of approximately about 4000 μm corresponds to an intermodal oscillation frequency of about 11.5 GHz for multi-mode laser. The effective SOA gain spectra bandwidth is 80 GHz due to limited bandwidth of DBR mirrors. The external EAM has a length of 200 μm and is used for optical amplitude control and suppression of various modes. The electrical wiring connections are also placed on the chip to provide DC biasing for SOA, PM and EAM. A ground (GND) pad is connected with via hole for ground access on the chip surface.
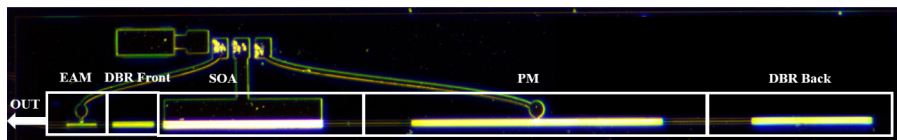

Fig. 2. Fabricated DBR based multi-mode multi-section semiconductor laser on InP chip with DC bias control gold pads in rectangular patterns.

The microchip placement on a temperature controlled environment is depicted in Fig. 3 for static and dynamic optical characterization, where mechanical probe-stations support electrical microprobe to provide necessary electrical (DC/RF) input and optical lensed fiber holder to collect optical output. A copper sheet is placed under the custom designed microchip and

mounted on a Peltier cooler for maintaining 20°C temperature throughout test environment using a thermistor and Temperature controller (Thorlabs TED8040) with temperature fluctuation of +/−0.2°C. The optical output of this laser under test is monitored on optical spectrum analyzer (Agilent MS9710C) through lensed fiber, optical coupler, and then photodiode to monitor RF characteristics. The PM bias and EAM bias is kept initially at 0.0V for initial performance measurement and static characterization. The measured test results of the integrated laser are shown in Table 1, where there are 5 dominant modes existing in multi-mode laser operation. The measured optical output power for the fundamental mode is around −12 dBm at 1550.85 nm, when SOA injection current is 80 mA. The mode gap between each mode is around 11.5 GHz, which matches well with estimated effective cavity length of 13.065 mm. Free running measurement of inter-modal output around 11.5 GHz is depicted in Fig. 4. The detected RF output power is about −10.59 dBm at 11.5496 GHz for SOA bias current of 80 mA and 0.0V bias voltages applied to PM and EAM sections. The spectral purity of intermodal oscillation is studied here and key performance is close-in to carrier phase noise and its related timing jitters. Measured close-in to carrier phase noise is depicted in Fig. 5, where a poor phase noise of −5 dBc/Hz at offset 1 kHz and −30 dBc/Hz at 10 kHz offset is recorded for the free-running inter-modal oscillation frequency. The max hold operation for 10 mins on this signal shows up to 30 MHz center frequency shift. The estimated timing jitter of this oscillator is 266.1 ps for 1 kHz to 1 MHz offset carrier frequencies.
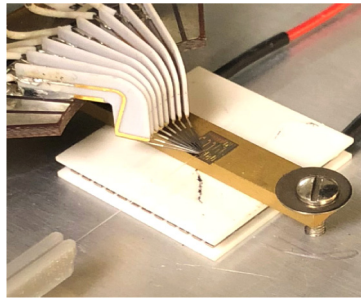

Fig. 3. Testing environment of the DBR based multi-mode multi-section semiconductor laser.
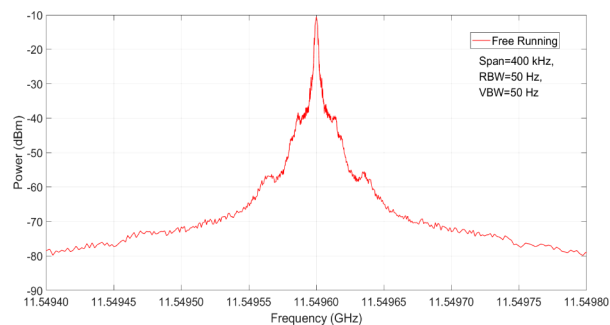
Fig. 4. Free-running performance of inter-modal RF output: center frequency of 11.5496 GHz with output power of −10.59 dBm, frequency span of 400 kHz, resolution bandwidth (RBW) of 50 Hz and video bandwidth (VBW) of 50 Hz.

The inter-modal RF frequency is tuned, when different DC injection voltage is applied to the PM section (cf. Fig. 2). The applied bias of −5.0V to + 1.0V to the PM section changes the index of refraction in the optical waveguide portion, causes a phase shift of 20°/mm to
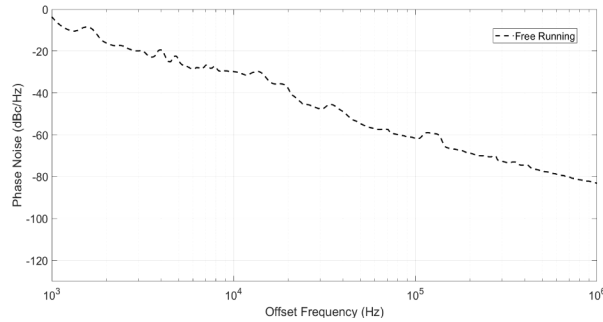
Fig. 5. Close-in to carrier phase noise over 1kHz to 1 MHz offset carrier frequency. A time averaging of 10 is used.

Table 1. Multi-mode laser output wavelength and related power level

Output modes	Wavelength (nm)	Power level (dBm)
1	1550.648	−30.1
2	1550.747	−21.3
3	1550.847	−12.3
4	1550.950	−19.5
5	1551.050	−36.2

17.5°/mm respectively, and changes the effective laser cavity length of the multi-section laser. The achieved phase shift and eventual change in the cavity length causes shift in the inert-modal oscillation frequency (i.e., adjusting mode gap) within multi-mode laser operation. Besides the static optical performance measurements, phase section tuning sensitivity is then measured for various PM biasing conditions. Table 2 summarizes the precise inter-modal results related to PM bias, which is over 800MHz at X-band with an average frequency tuning sensitivity of around 150 MHz/V. This achieved tuning range and sensitivity is among the best reported compared to other techniques and is significantly larger than conventional RF voltage controlled oscillator (VCO) tuning sensitivity [30].

Table 2. PM tuning sensitivity and RF output frequency versus DC bias of DBR laser PM section

DC bias of PM	Output frequency (GHz)	PM sensitivity (MHz/V)
−5.0 V	12.2725	189.5
−4.5 V	12.1827	179.5
−4.0 V	12.0975	170.3
−3.5 V	12.0159	163.2
−3.0 V	11.9382	155.3
−2.5 V	11.8647	147.0
−2.0 V	11.7949	139.5
−1.5 V	11.7288	132.1
−1.0 V	11.6659	125.8
−0.5 V	11.6062	119.4
0.0 V	11.5496	113.2
+0.5 V	11.4964	106.4
+1.0 V	11.4462	100.3

3. Self-forced oscillation techniques

In order to improve free-running oscillation frequency, the concept of forced oscillation is employed. Frequency stabilization using external frequency reference is reported [21], when a stable source is available; however a self-forced oscillation is useful when constructing a clean frequency Ref. [3] that is to be used as an external reference for stabilization of distributed oscillators [31]. In a similar manner to a modular forced OEO design, forced technique of SIL, SPLL, and SILPLL are then incorporated to this semiconductor laser system to stabilize inter-modal oscillation frequency and reduce its phase noise performance.

The conceptual block diagram of SIL [27] using control theory representation is shown in Fig. 6. A portion of the oscillator output signal is delayed by a long delay (τ_d) and is fed back to the oscillator with coupling factor of ρ. The phase of the delayed signal is then compared against that of current signal to generate an error signal for self-injection to the oscillator.
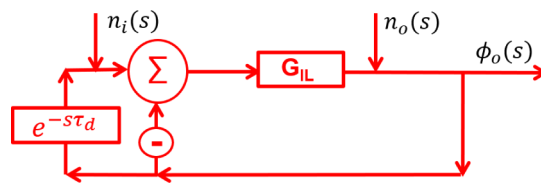
Fig. 6. Conceptual block diagram of SIL using control theory representation with a self-feedback after a delay of Td with coupling factor of ρ integrated to system [27].

The phase noise of self-injection locking system is expressed as Eq. 1:

$$S_{SIL}(\omega_m) = |H_{SIL}(s)|^2 S_{n_i}(\omega_m) + |HE_{SIL}(s)|^2 S_{n_o}(\omega_m), \tag{1}$$

where

$$H_{SIL}(S) = \frac{G_{IL}}{(1 - e^{-s\tau_d})G_{IL} + 1}, HE_{SIL}(S) = \frac{1}{(1 - e^{-s\tau_d})G_{IL} + 1}. \tag{2}$$

In Eq. 1, S_{ni}, S_{n0} are the residual noise of the system and oscillator phase noise separately. It is obvious that, when the gain of the system is high enough, the phase noise introduced by original oscillator will get significantly reduced.

The concept diagram of self-phase locking [28] is in similar manner in Fig. 7 besides the black dotted square, which representing the frequency discriminator. In SPLL process, a portion of the oscillator output is being delayed and the phase of the delayed signal is compared against the phase of the current signal. The comparison results will be then amplified by operational amplifier and provide feedback to the VCO tuning port. The feedback is initially a low deviation frequency (i.e., AC) signal and eventually reaches DC status, when no phase error detected between the delayed and non-delayed signals.
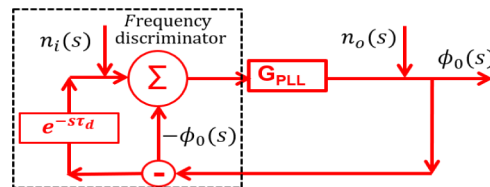
Fig. 7. Control theory representation of SPLL [28].

With method of superposition principle applied, overall noise of the SPLL system is:

$$S_{SPLL}(\omega_m) = |H_{SPLL}(s)|^2 S_{n_i}(\omega_m) + |HE_{SPLL}(s)|^2 S_{n_o}(\omega_m), \tag{3}$$

where

$$H_{SPLL}(S) = \frac{G_{PLL}}{(1 - e^{-s\tau_d})G_{PLL} + 1}, HE_{SPLL}(S) = \frac{1}{(1 - e^{-s\tau_d})G_{PLL} + 1}. \tag{4}$$

Combining SIL and SPLL lead to SILPLL with a similar simplified expression [32]. Related conceptual diagram is depicted in Fig. 8.
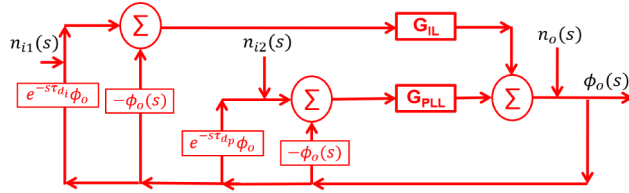

Fig. 8. Control theory representation of SILPLL [32].

In this topology, SIL and SPLL are conducted at the same time with separate external delay circuits. The derived expression using superposition principle is:

$$S_{\Phi_0} = \left| \frac{G_{IL} + G_{PLL}}{1 + K_{IL}G_{IL} + K_{PLL}G_{PLL}} \right|^2 S_{n_i} + \left| \frac{1}{1 + K_{IL}G_{IL} + K_{PLL}G_{PLL}} \right|^2 S_{n_0}, \tag{5}$$

where

$$K_{IL} = 1 - e^{-s\tau_{d_i}}, K_{PLL} = 1 - e^{-s\tau_{dp}}. \tag{6}$$

The analytical expression of Eq. 5 signifies that SIL, SPLL and their combination both can provide significantly phase noise reduction without use of any external reference. Meantime, in order to better optimize semiconductor laser based system, the self-forced operation parameters are to be identified, as discussed in next part.

The test set-up diagram of self-injection locking is depicted in Fig. 9, where the instantaneous laser output is amplified using a constant gain erbium doped fiber amplifier (EDFA), delayed (25 µs using 5km fiber), and fed back to laser through an optical circulator. A tunable optical attenuator is placed before an optical circulator port for evaluating dynamic performance by adjusting optical injection power levels that are verified using optical power meter (EXFO FPM-600). There is a polarization controller (PC) after optical delay line in order to provide high efficiency optical injection signal to the optical waveguide. The inter-modal RF oscillation is measured using RF phase noise analyzer (Rohde-Schwarz FSWP-26).
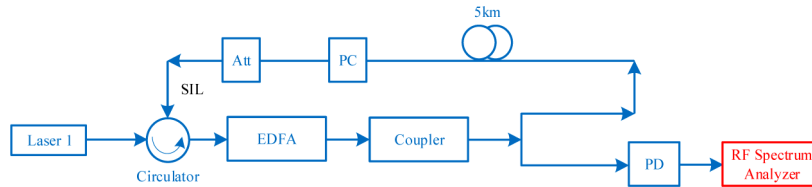

Fig. 9. Block diagram of self-injection locking system with electrical system designated in red color, while optical system is in blue color.

Phase noise performance comparison of free-running intermodal oscillation with SIL under various injected optical levels are presented in Fig. 10(a), where significant reduction in phase

noise is observed with P_{inj}/P_o=0.3 ratio (i.e., SIL power of −10 dBm after optical attenuator, the coupling loss of lensed fiber to waveguide is 6 dB). It provides the best phase noise performance among other situations with level of −40 dBc/Hz (i.e., 35 dB reduction with free running) at 1 kHz offset and −80 dBc/Hz (50 dB reductions with free running) at 10 kHz. On the other hand, phase noise performances of forced SIL are also compared in Fig. 10(b) in order to quantify the best optical delay length. Nonetheless, 5 km delay lines provides the best phase noise performance using optimized power injection power ratio among several different delay lines. Meantime, the best achieved timing jitter is 5.17 ps which is 50 times better than free running case for offset frequencies of 1 kHz to 1 MHz. From Fig. 10(a), side-modes at harmonics of 40kHz are distinctly visible, which are due to 25 μs delay time of injection loop, which contributes to timing jitters of RF reference. A similar side-mode peaks are also seen in Fig. 10(b), which is related to round trip time delay of various fiber delay lengths of 1-7 km. These side-modes introduce degradation in timing jitters and are to be reduced using either dual feedback loop of DSIL [27] or combination of SILPLL [29]. Moreover, single or multiple delayed self-phase lock loop of SPLL technique [28] reduce the phase noise further and at the same time reduce the side mode peak observed in SIL case.
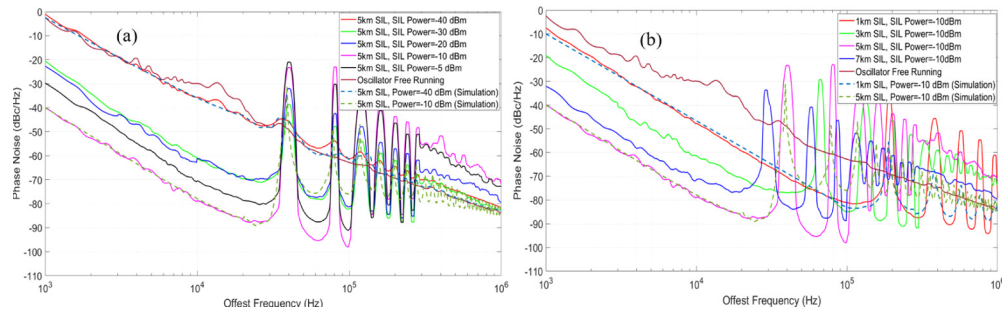
Fig. 10. Phase noise performance comparison of self-injection locking with free-running inter-modal oscillation, a) different injection power levels, b) different fiber delay line lengths.

The core component of phase locked loop (PLL) function is an integrated low pass filter and mixer board for phase error detection between instantaneous signal and a reference (either external or a delayed version of instantaneous signal). The design concept and related description is reported in [28]. The phase detector is realized using an X-band mixer combined with a lowpass filter amplifier (i.e., Mixer + LPFA board of Fig. 11). A 50 MHz loop bandwidth PLL board is redesigned accordingly in this paper because the nature variation of the inter-modal output is between 30-35 MHz at fixed temperature of 20°C. Therefore, the loop bandwidth of operational amplifier on PLL board needs to cover whole potential frequency variation in order to maintain phase locking status. The design of phase detection board is optimized based on phase locking performance using an external frequency reference (Gigatronics GT 9000 frequency synthesizer). The block diagram of phase locking function is depicted in Fig. 11. The RF synthesizer works as the reference source to lock laser inter-modal output with the help of PLL board. If any phase error is detected between reference signal and inter-modal oscillation, a frequency tuning voltage signal is fed back to the PM section to lock the free-running oscillation frequency to the reference signal. The frequency locking range is recorded in Table 3 for 50 MHz loop bandwidth. The external phase locking circuit lost locking status when frequency difference is 53 MHz, which is out of the loop bandwidth range; effectively this PLL board can successfully provide phase locking, if the instantaneous RF frequency variation is within 50 MHz.

The phase noise performance of external phase locking is provided in Fig. 12. The PLL locked RF signal quality get significant improvement compared with free-running and its phase noise in close in to the carrier is forced to follow the external reference characteristics. Its related phase
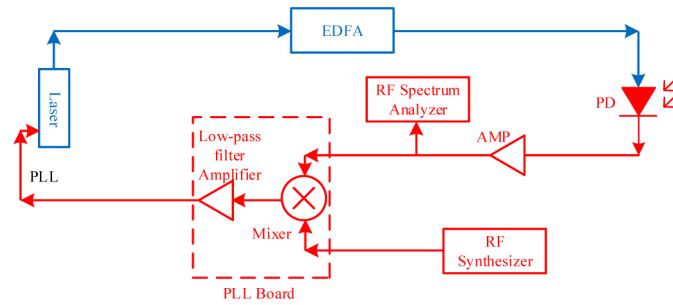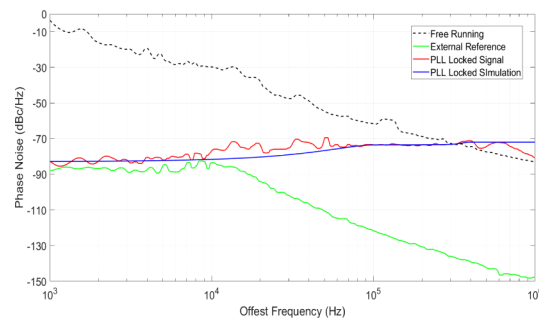
Fig. 11. External phase locking set-up using external frequency reference from RF synthesizer by detection of phase error is detected and used to control PM section of multi-section laser.

Table 3. PLL board locking range testing using external RF synthesizer source for loop bandwith of 50 MHz

Laser frequency (GHz)	Reference frequency (GHz)	Locking?	Frequency shift (after 10 mins)
11.540	11.540	Yes	<5 kHz
11.540	11.550	Yes	<5 kHz
11.540	11.560	Yes	<5 kHz
11.540	11.570	Yes	<5 kHz
11.540	11.580	Yes	<5 kHz
11.540	11.585	Yes	<5 kHz
11.540	11.590	Yes	<5 kHz
11.540	11.593	No	Shifting

noise is −85 dBc/Hz at 1kHz and 10 kHz offset, which is phase locked by forced PLL using external microwave reference signal. This phase noise performance is unchanged no matter what reference signal frequency is used as long as it is within 50 MHz locking range. Moreover, the stability performance is significantly improved as well. The frequency shift is reduced from 30 MHz to less than 5 kHz during 10 mins period.

Fig. 12. Phase noise performance using external phase locking circuit (RF frequency of 11.54 GHz, RF output Power of 5.39 dBm).

After evaluating optimum operation of PLL functions, performance of injection locking and phase locking combination is further studied in order to combine them together. One of important benefits of combining IL and PLL is its added benefit in pull-in time [33]. The pull-in time is used to describe how long it takes for signal with initial frequency error with reference to reach a

steady status of zero frequency error; this figure of merit is measured using external reference synthesizer signal. Related expression for PLL and ILPLL pull-in time is provided in Eq. 7 and Eq. 8 [33], where $\Delta\omega_0$ is frequency difference between inter-modal output and reference signal, ω_n is nature frequency, $\Delta\omega_i$ is locking range, and K is open loop gain. Meantime, according to [33], higher loop gain will also bring better phase noise performance. Open loop gain as high as 92 dB will introduce 10 dB phase noise reduction when comparing with 72 dB loop gain case.

$$\frac{(\Delta\omega_0)^2}{\omega_n^2 K}, \tag{7}$$

$$\frac{\Delta\omega_0^2 - (\Delta\omega_i)^2}{\omega_n^2 \Delta\omega_i}. \tag{8}$$

Comparison of the measured and simulated results is depicted in Fig. 13 for different PM offset biasing. From Fig. 13, ILPLL will provide at least 20 times faster pull-in time compared with PLL only. In addition, a smaller negative offset reverse bias voltage of PM (i.e., a larger absolute value) provides a faster pull-in time compared with larger negative offset voltage (i.e., a smaller absolute value).
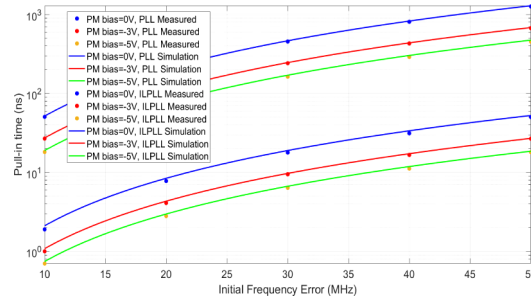
Fig. 13. Simulation and measurement results of pull-in time of PLL and ILPLL using the external frequency reference.

Optimized performance of PLL and ILPLL in term of locking range, pull-in time is used for combination of SIL and SPLL as developed in Fig. 14. The SIL part is still kept the same while SPLL [28] part is realized by multiple delay lines to function as the reference signal in order to remove the need of external synthesizer reference in PLL structure. The high Q and energy storage characteristic of long optical delay line provides a delayed reference for self-stabilization of instantaneous inter-modal oscillation. The delayed and non-delayed signals are simultaneously compared using the optimized phase detector (i.e., Mixer + LPFA board of Fig. 14). Any instantaneous phase error is then detected and the low frequency component is filtered as a frequency tuning signal and feedback to PM of the semiconductor laser. This phase comparison of delayed and instantaneous signal pulls back the frequency deviation to original oscillation frequency (i.e., delayed signal as reference), which is the process of phase lock loop (PLL). Since the natural variation of free running laser inter-modal RF output is within 30 MHz at 20°C, the PLL board loop bandwidth of 50 MHz is sufficient in order to completely cover any potential shift. Large phase tuning sensitivity of PM (an average sensitivity of 150 MHz/V), the low frequency feedback scan range is then set at a maximum voltage swing of −1.0V to + 1.0V, which is sufficient to correct maximum 30 MHz frequency drift. Finally, the output of PLL board becomes a constant DC voltage when inter-modal oscillator is locked.

Different offset bias conditions of PM section are also compared using optimized self-injection locking 5km and triple self-phase locking 500m, 1km, and 3km to test its related phase noise performance. Triple non-harmonically related delay loop [29] suppresses most effectively peaks
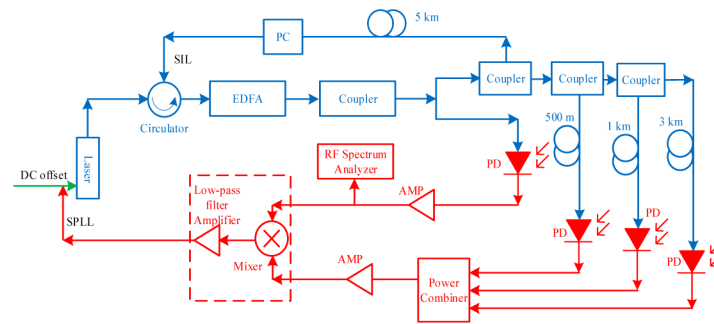
Fig. 14. Block diagram of inter-modal oscillation stabilization using a combination of self-injection locking (SIL) and triple self-phase locking (TSPLL).

of side modes generated by self-injection locking. In fact, all the significant side mode peaks are effectively suppressed (from –30 dBc to –90 dBc) compared with self-injection locking case because of multiple loops. Moreover, shorter SPLL delay line will contribute to fast phase locking speed [33]. From the measurement results in Fig. 15, PM bias of 0 V provides the best phase noise results of −58 dBc/Hz at 1 kHz offset and −98 dBc/Hz at 10 kHz offset by avoiding any DC bias for PM. The phase noise performance comparing with free running case shows reduction of 53 dB at 1 kHz offset and 68 dB at 10 kHz offset which also matches well with simulation prediction in Fig. 15. In the best scenario, the achieved timing jitter is 0.448 ps which is 600 times better than free running conditions.
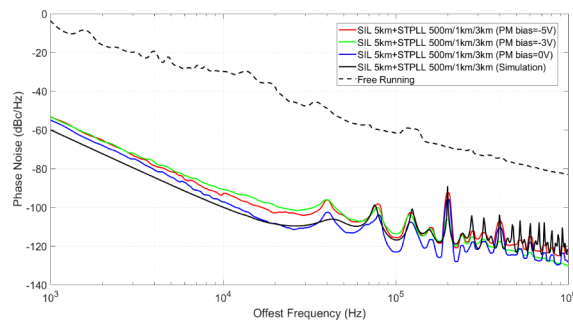
Fig. 15. Phase noise performance of SILPLL based inter-modal RF output and comparison to simulated results under different PM bias while free-running is depicted for comparison (RF = 11.54 GHz, RF Power = 3.59 dBm).

4. Discussions and conclusions

The designed multi-section multi-mode laser shows generation of inter-modal oscillation at RF frequencies of X-band. The PM section controls RF performance in terms of frequency tuning and phase noise reduction using SPLL technique. This process of self-forced oscillation using SPLL is combined with SIL to achieve SILPLL based stabilization without any external reference. The measured 11.5 GHz RF output signal with phase noise of −58 dBc/Hz at offset 1 kHz and −98 dBc/Hz at offset 10 kHz is generated using self-reference technique. These results are excellent even compared with the previously reported [14–16] using external RF reference. In fact, it is the first time that inter-modal oscillation of monolithically integrated multi-mode laser is reported with significant frequency stabilization that leads to calculated timing jitters of under 0.5ps at 11.5 GHz. The success of applied forced technique also shows great potential for higher

frequency generation using larger mode gap and larger modes number laser design, where stable external reference are not available. The existing delay element of optical fiber could be replaced by high quality factor integrated resonators [34,35]. In conclusion, it is very promising to further use the proposed SILPLL based inter-modal multi-mode semiconductor lasers for building up compact millimeter wave synthesizers.

Funding

References

1. S. Ye, L. Jansson, and I. Galton, "A multiple-crystal interface PLL with VCO realignment to reduce phase noise," IEEE J. Solid-State Circuits **37**(12), 1795–1803 (2002).
2. A. S. Daryoush, *Microwave Photonics from Components to Applications and Systems* (Springer Science & Business Media, 2003), Chap. 6.
3. A. K. Poddar, U. L. Rohde, and A. S. Daryoush, "Self-Injection Locked Phase Locked Loop Optoelectronic Oscillator," WO Patent, WO2014105707A1, (2014).
4. T. Sun, L. Zhang, A. K. Poddar, U. L. Rohde, and A. S. Daryoush, "Forced SILPLL oscillation of X- and K-band frequency synthesized opto-electronic oscillators," in *Proceedings of IEEE Conference on International Topical Meeting on Microwave Photonics* (IEEE, 2016), pp. 91–94.
5. T. Sun, L. Zhang, A. K. Poddar, U. L. Rohde, and A. S. Daryoush, "Frequency synthesis of forced opto-electronic oscillators at the X-band," Chin. Opt. Lett. **15**(1), 10009–10013 (2017).
6. T. Sun, A. S. Daryoush, A. Poddar, L. Zhang, and U. Rohde, "High-resolution frequency synthesizers over X-band using SILPLL opto-electronic oscillators," in *Proceedings of Joint Conference of the European Frequency and Time Forum and IEEE International Frequency Control Symposium* (IEEE, 2017), pp. 484–485.
7. G. Pillet, L. Morvan, D. Dolfi, J. Schiellein, and T. Merlet, "Stabilization of new generation solid-state dual-frequency laser at 1.5 μm for optical distribution of high purity microwave signals," in *Proceedings of IEEE Conference on International Topical Meeting on Microwave Photonics* (IEEE, 2010), pp. 163–166.
8. G. Pillet, L. Morvan, M. Brunel, F. Bretenaker, D. Dolfi, M. Vallet, J. P. Huignard, and A. L. Floch, "Dual-Frequency Laser at 1.5 μm for Optical Distribution and Generation of High-Purity Microwave Signals," J. Lightwave Technol. **26**(15), 2764–2773 (2008).
9. T. D. Ni, X. Zhang, and A. S. Daryoush, "Close-in carrier phase noise of laser with coherent feedback," in *Proceedings of IEEE Conference on International Microwave Symposium Digest* (IEEE, 1994), pp. 61–64.
10. T. D. Ni, X. Zhang, and A. S. Daryoush, "Experimental Study on Close-in carrier Phase Noise of Laser Diode with Coherent Feedback," IEEE Trans. Microwave Theory Tech. **43**(9), 2277–2283 (1995).
11. W. Zhang and J. Yao, "A silicon photonic integrated frequency-tunable optoelectronic oscillator," in *Proceedings of IEEE Conference on International Topical Meeting on Microwave Photonics* (IEEE, 2017), pp. 1–4.
12. G. Carpintero, S. Hisatake, D. Felipe, R. Guzman, T. Nagatsuma, N. Keil, and T. Gobel, "Photonics-based millimeter and terahertz wave generation using a hybrid integrated dual DBR polymer laser," in *Proceedings of IEEE Conference on International Microwave Symposium* (IEEE, 2016), pp. 1–3.
13. F. Dijk, M. Lamponi, M. Chtioui, F. Lelarge, G. Kervella, E. Rouvalis, C. Renaud, M. Fice, and G. Carpintero, "Heterodyne millimeter wave source with monolithically integrated UTC photodiodes," in *Proceedings of IEEE Conference on International Topical Meeting on Microwave Photonics* (IEEE, 2013), pp. 336–339.
14. G. Carpintero, M. G. Thompson, R. V. Penty, and I. H. White, "Low Noise Performance of Passively Mode-Locked 10-GHz Quantum-Dot Laser Diode," IEEE Photonics Technol. Lett. **21**(6), 389–391 (2009).
15. F. Quinlan, S. Ozharar, S. Gee, and P. J. Delfyett, "Harmonically modelocked semiconductor based lasers as high repetition rate ultralow noise pulse train and optical frequency comb sources," J. Opt. A: Pure Appl. Opt. **11**(10), 103001 (2009).
16. A. Ishizawa, T. Nishikawa, A. Mizutori, H. Takara, A. Takada, T. Sogawa, and M. Koga, "Phase-noise characteristics of a 25-GHz-spaced optical frequency comb based on a phase- and intensity-modulated laser," Opt. Express **21**(24), 29186–29194 (2013).
17. I. Morohashi, T. Sakamoto, H. Sotobayashi, T. Kawanishi, I. Hosako, and M. Tsuchiya, "Widely repetition-tunable 200 fs pulse source using a Mach–Zehnder-modulator-based flat comb generator and dispersion-flattened dispersion-decreasing fiber," Opt. Lett. **33**(11), 1192–1194 (2008).
18. S. Arahira and Y. Ogawa, "40 GHz actively mode-locked distributed bragg reflector laser diode module with an impedance-matching circuit for effi- cient RF signal injection," Jpn. J. Appl. Phys. **43**(4B), 1960–1964 (2004).
19. L. Hou, R. Dylewicz, M. Haji, P. Stolarz, B. Qiu, and A. C. Bryce, "Monolithic 40-GHz Passively Mode-Locked AlGaInAs–InP 1.55-um MQW Laser With Surface-Etched Distributed Bragg Reflector," IEEE Photonics Technol. Lett. **22**(20), 1503–1505 (2010).
20. T. Hoshida, H. Liu, M. Tsuchiya, Y. Ogawa, and T. Kamiya, "Subharmonic hybrid mode-locking of a monolithic semiconductor laser," IEEE J. Sel. Top. Quantum Electron. **2**(3), 514–522 (1996).

21. A. S. Daryoush, K. Sato, K. Horikawa, and H. Ogawa, "Electrically injection-locked intermodal oscillation in a long optical cavity laser diode," IEEE Microw. Guid. Wave Lett. **7**(7), 194–196 (1997).

22. A. S. Daryoush, K. Sato, K. Horikawa, and H. Ogawa, "Dynamic response of long optical-cavity laser diode for Ka-band communication satellites," IEEE Trans. Microwave Theory Tech. **45**(8), 1288–1295 (1997).

23. V. Kroeze, "SmartPhotonics Introduction," https://smartphotonics.nl/.

24. L. A. Johansson, Y. A. Akulova, G. A. Fish, and L. A. Coldren, "Sampled-grating DBR laser integrated with SOA and tandem electroabsorption modulator for chirp-control," Electron. Lett. **40**(1), 70–71 (2004).

25. S. Joshi, C. Calò, N. Chimot, M. Radziunas, R. Arkhipov, S. Barbet, A. Accard, A. Ramdane, and F. Lelarge, "Quantum dash based single section mode locked lasers for photonic integrated circuits," Opt. Express **22**(9), 11254–11266 (2014).

26. J. S. Barton, E. J. Skogen, M. L. Masanovic, S. P. Denbaars, and L. A. Coldren, "A widely tunable high-speed transmitter using an integrated SGDBR laser-semiconductor optical amplifier and Mach-Zehnder modulator," IEEE J. Sel. Top. Quantum Electron. **9**(5), 1113–1117 (2003).

27. L. Zhang, A. K. Poddar, U. L. Rohde, and A. S. Daryoush, "Analytical and experimental evaluation of SSB phase noise reduction in self-injection locked oscillators using optical delay loops," IEEE Photonics J. **5**(6), 6602217 (2013).

28. L. Zhang, A. K. Poddar, U. L. Rohde, and A. S. Daryoush, "Comparison of optical self-phase locked loop techniques for frequency stabilization of oscillators," IEEE Photonics J. **6**(5), 1–15 (2014).

29. T. Sun, L. Zhang, A. K. Poddar, U. L. Rohde, and A. S. Daryoush, "Limits in Timing Jitters of Forced Microwave Oscillator Using Optical Self-ILPLL," IEEE Photonics Technol. Lett. **29**(2), 181–184 (2017).

30. M. Chen and J. Xu, "Wideband Frequency Synthesizer at X/Ku Band by Mixing and Phase Locking of Half Frequency Output of VCO," J. Infrared, Millimeter, Terahertz Waves **31**(1), 100–110 (2009).

31. A. S. Daryoush, "Optical synchronization of millimeter-wave oscillators for distributed architecture," IEEE Trans. Microwave Theory Tech. **38**(5), 467–476 (1990).

32. L. Zhang, *Optoelectronic frequency stabilization techniques in forced oscillators* (Ph.D. Dissertation, 2014).

33. J. Lin, *Study of Digital Fiber-Optic Link and Clock Recovery Circuit at 1.25Gb/s*, (Ph.D. Dissertation, 1995).

34. G. Karen, *Optical whispering-gallery mode resonators for applications in optical communication and frequency control* (Ph.D. Dissertation, 2013).

35. A. A. Savchenkov, V. S. Iichenko, J. Byrd, W. Liang, D. Eliyahu, A. B. Matsko, D. Seidel, and L. Maleki, "Whispering-gallery mode based opto-electronic oscillators," in *Proceedings of IEEE Conference on International Frequency Control Symposium* (IEEE, 2010), pp. 554–557.